

# An Essential Esterase (BroH) for the Mineralization of Bromoxynil Octanoate by a Natural Consortium of *Sphingopyxis* sp. Strain OB-3 and *Comamonas* sp. Strain 7D-2

Kai Chen, Yuan Liu, Dong-Mei Mao, Xiao-Mei Liu, Shun-Peng Li, and Jian-Dong Jiang\*

Department of Microbiology, Key Lab of Microbiological Engineering of Agricultural Environment, Ministry of Agriculture, College of Life Sciences, Nanjing Agricultural University, 210095 Nanjing, People's Republic of China

**ABSTRACT:** A natural consortium of two bacterial strains (*Sphingopyxis* sp. OB-3 and *Comamonas* sp. 7D-2) was capable of utilizing bromoxynil octanoate as the sole source of carbon for its growth. Strain OB-3 was able to convert bromoxynil octanoate to bromoxynil but could not use the eight-carbon side chain as its sole carbon source. Strain 7D-2 could not degrade bromoxynil octanoate, although it was able to mineralize bromoxynil. An esterase (BroH) that is involved in the conversion of bromoxynil octanoate into bromoxynil and is essential for the mineralization of bromoxynil octanoate by the consortium was isolated from strain OB-3 and molecularly characterized. BroH encodes 304 amino acids and resembles  $\alpha/\beta$ -hydrolase fold proteins. Recombinant BroH was overexpressed in *Escherichia coli* BL21 (DE3) and purified by Ni-NTA affinity chromatography. BroH was able to transform *p*-nitrophenyl esters (C2–C14) and showed the highest activity toward *p*-nitrophenyl caproate (C6) on the basis of the catalytic efficiency value ( $V_{\max}/K_m$ ). Additionally, BroH activity decreased when the aliphatic chain length increased. The optimal temperature and pH for BroH activity was found to be 35 °C and 7.5, respectively. On the basis of a phylogenetic analysis, BroH belongs to subfamily V of bacterial lipolytic enzymes.

**KEYWORDS:** consortium, esterase (BroH), bromoxynil octanoate, bromoxynil, *Sphingopyxis* sp. OB-3, *Comamonas* sp. 7D-2

## ■ INTRODUCTION

Herbicides are broadly used in agriculture and on golf courses, utility corridors, and residential and other lands. However, misuse or overuse of these chemicals can have considerable environmental and public health consequences. Bromoxynil octanoate (2,6-dibromo-4-cyanophenyl octanoate) is a contact herbicide that acts by inhibiting photosynthesis specifically in weeds with broad leaves.<sup>1</sup> Bromoxynil (3,5-dibromo-4-hydroxybenzonitrile), the octanoate ester hydrolyzate of bromoxynil octanoate, is another herbicide that is used to control broad-leaved weeds.<sup>2</sup> Although these two herbicides have relatively short half-lives (generally less than 1 month), their extensive use has resulted in environmental pollution and ecosystem damage.<sup>3,4</sup> Previous studies of toxicity and ecological risk have shown that green algal species are extremely sensitive to bromoxynil octanoate, which renders it a threat to aquatic ecosystems.<sup>5</sup> Bromoxynil is a suspected teratogen and can be highly toxic to moderately toxic to freshwater fish. Because both bromoxynil octanoate and bromoxynil are harmful to ecosystems and human health, it is important to examine the dissipation of these two herbicides in the environment. One previous study that examined metabolic pathways in <sup>14</sup>C-labeled wheat found that bromoxynil octanoate was first hydrolyzed to bromoxynil and then either consecutively or concurrently underwent debromination, deamination, and hydrolysis.<sup>6</sup> Furthermore, the degradation of <sup>14</sup>C-labeled bromoxynil octanoate has been reported in sandy loam soil with a half-life of 2 days. The major degradation product was determined to be CO<sub>2</sub>, which accounted for 64.28% of the radioactivity detected after 90 days. Although hydrolysis and photolytic degradation both play a role in the dissipation of bromoxynil octanoate, microbially mediated degradation is the most important environmental process for this compound.

The degradation of bromoxynil octanoate by pure microbial cultures has not been extensively studied. Thus far, the only strain that has been reported to be capable of transforming bromoxynil octanoate to bromoxynil and then to 3-bromo-4-hydroxybenzoate via 3,5-dibromo-4-hydroxybenzoate is *Acinetobacter* sp. strain XB2.<sup>7</sup> Although microorganisms capable of degrading bromoxynil have been isolated in the past,<sup>1,8</sup> the mineralization of bromoxynil octanoate by a consortium of bacteria has never been reported, and the esterase involved in the conversion of bromoxynil octanoate into bromoxynil has not been identified.

This study elucidated the synergistic roles of two bacterial strains that comprise a natural consortium in the degradation of bromoxynil octanoate and molecularly characterized an esterase, BroH, that is involved in the conversion of bromoxynil octanoate into bromoxynil and is essential for the mineralization of bromoxynil octanoate by the consortium.

## ■ MATERIALS AND METHODS

**Chemicals and Media.** Bromoxynil octanoate (>98% purity) and bromoxynil (>98% purity) were purchased from J&K Chemical Co., Ltd. (Shanghai, People's Republic of China). *p*-Nitrophenyl acetate (C2), *p*-nitrophenyl caprate (C10), and *p*-nitrophenyl myristate (C14) were purchased from Sigma-Aldrich (St. Louis, MO, USA). *p*-Nitrophenyl butyrate (C4), *p*-nitrophenyl caproate (C6), *p*-nitrophenyl octanoate (C8), *p*-nitrophenyl laurate (C12), and *p*-nitrophenyl palmitate (C16) were purchased from Tokyo Chemical Industry Co.,

**Received:** August 27, 2013

**Revised:** November 11, 2013

**Accepted:** November 13, 2013

**Published:** November 13, 2013

Ltd., Japan. Diethyl pyrocarbonate (DEPC), iodoacetamide, Tween-20, Tween-80, sodium dodecylsulfate (SDS), Triton X-100, and phenylmethylsulfonyl fluoride (PMSF) were purchased from GENETIME Biotechnology Co., Ltd., People's Republic of China. All molecular biology reagents were purchased from TaKaRa Biotechnology (Dalian) Co., Ltd.

Luria–Bertani (LB) and mineral salt medium (MM; 1.0 g of  $\text{NH}_4\text{NO}_3$ , 1.6 g of  $\text{K}_2\text{HPO}_4$ , 0.5 g of  $\text{KH}_2\text{PO}_4$ , 0.2 g of  $\text{MgSO}_4$  and 1.0 g of  $\text{NaCl}$  per liter of water, pH 7.0) were both used in this study. MM was supplemented with 100 mg/L bromoxynil octanoate (MMBO) or 100 mg/L bromoxynil (MMB). Solid medium was prepared by adding 2.0% (w/v) agar. When strains carrying antibiotic resistance markers were cultured, the medium was supplemented with 100 mg/L ampicillin (Amp), 50 mg/L kanamycin (Km), or 80 mg/L gentamicin (Gm) as necessary.

**Characterization of Two Bacterial Strains in a Bromoxynil Octanoate Degrading Consortium.** The isolation of the bromoxynil octanoate degrading consortium has been described previously.<sup>9</sup> Colonies were tested for the ability to degrade bromoxynil octanoate by ultraviolet scanning and were further analyzed by high-performance liquid chromatography (HPLC) as described below. One colorless and flat colony, which appeared on MMBO agar after 24 h, was highly efficient in degrading bromoxynil octanoate. This colony was further purified by repetitive streaking on LB agar. Interestingly, after 60 h of cultivation, another small, light yellow, and convex colony appeared in the previously colorless colony. In the end, two bacterial strains, designated as OB-3 and 7D-2, were purified from each of these colonies. The two strains were identified on the basis of their morphological, physiological, and biochemical properties as described in *Bergey's Manual of Determinative Bacteriology* as well as their 16S rRNA gene sequence analysis. The 16S rRNA gene was amplified by a previously described PCR method.<sup>10</sup> The nucleotide sequences coding for the 16S rRNA of strain OB-3 (1,369 bp) and 7D-2 (1,491 bp) were deposited in the GenBank database under the accession numbers JN797629 and JX455142, respectively. Alignment of the different 16S rRNA gene sequences from the GenBank database was performed using Clustal X 1.8.3 with default settings.<sup>11</sup> Phylogeny was analyzed with MEGA version 4.0 software,<sup>12</sup> and distances were calculated using the Kimura 2 parameter distance model.

**Synergistic Degradation and Growth of the Consortium.** To investigate the synergistic relationship between strains OB-3 and 7D-2, their growth and their ability to degrade bromoxynil octanoate/bromoxynil were examined. Both strains were precultured in LB medium containing either 50 mg/L of bromoxynil octanoate or 50 mg/L of bromoxynil until they reached midlog phase. The cells were then harvested by centrifugation at 6000g for 5 min and washed three times with sterilized  $\text{H}_2\text{O}$ . Next, the cell density was determined by the  $\text{OD}_{600\text{ nm}}$  value. After the cell density was adjusted to 1.0, the cultures were inoculated into 100 mL of MMBO or MMB at 5% v/v. In a separate degradation experiment, each strain was inoculated individually in contrast to the simultaneous inoculation in the mixed degradation experiment. All cultures were incubated at 30 °C and 150 rpm. The concentration of bromoxynil was analyzed by high-performance liquid chromatography (HPLC) at an interval of 12 h. Because of its lower solubility and heterogeneity in the medium, the concentration of bromoxynil octanoate was only determined at the end of the experiment. Because strain 7D-2 grows fast and forms colorless and flat colonies on LB plates at 24 h, while strain OB-3 grows slowly and forms light yellow and convex colonies only after 60 h, the number of cells in each strain was counted separately by the plate counting method. All of the treatment conditions were replicated three times.

**Bromoxynil Octanoate and Bromoxynil Analysis.** Bromoxynil octanoate and bromoxynil were extracted from the medium with an equal volume of dichloromethane. The extract was dried over anhydrous  $\text{Na}_2\text{SO}_4$  and evaporated using a vacuum rotary evaporator at room temperature. The residue was dissolved in 1 mL of methanol and analyzed by HPLC (600 controller, Rheodyne 7725i manual injector, and 2487 Dual  $\lambda$  Absorbance Detector; Waters Co., Milford, MA). The Kromasil 100-5  $\text{C}_{18}$  stationary phase was used in the separation column (4.6 mm internal diameter and 250 mm length). To analyze bromoxynil

octanoate, the mobile phase was pure methanol, and the flow rate was 0.8 mL/min. In contrast, to analyze bromoxynil, the mobile phase was acetonitrile/water/acetic acid (50/50/0.5, v/v/v), and the flow rate was the same. Bromoxynil octanoate and bromoxynil were simultaneously detected at 221 and 250 nm, respectively, and the concentration was determined from the peak area ratio relative to individual standard calibration curves.

**Identification of the Metabolite Produced from Bromoxynil Octanoate by Strain OB-3.** Cells from strain OB-3 were inoculated at 2% (v/v) into 20 mL of MMBO with 10 mM glucose and incubated at 30 °C and 150 rpm for 3 days. As a negative control, the inoculated cells were first heat-killed before being subjected to the same conditions. The samples were extracted similarly as described above and identified by gas chromatography–mass spectrometry (GC-MS). GC-MS analyses were performed on a Thermo Trace DSQ mass spectrometer under the following conditions. Helium was used as carrier gas at a flow rate of 1.2 mL/min. Gas chromatography was conducted using a RTX-SMS column (15 m  $\times$  0.25 mm  $\times$  0.25  $\mu\text{m}$ , Restek Corp., USA). The column temperature program began at 50 °C for 1 min, increased to 200 °C at 50 °C/min and held for 1 min, and then increased to 250 °C at 5 °C/min and held for 1 min. The injector temperature was set at 220 °C with a split ratio of 20/1. Both the interface temperature and ion source temperature were set at 250 °C. The column outlet was inserted directly into the electron ionization source block and operated at 70 eV.

**Cloning and Sequence Analysis of the Bromoxynil Octanoate Hydrolyzing Esterase Gene.** DNA manipulation was carried out as previously described by Sambrook and Russell.<sup>13</sup> Genomic DNA from *Sphingopyxis* sp. OB-3 was partially digested by a *Sau3AI* restriction digest. The resulting 3–5 kb DNA fragments were cloned into *Bam*HI-digested pUC118 (Takara, Dalian, People's Republic of China) and introduced into *E. coli* DH5 $\alpha$ .<sup>14</sup> The transformants were plated onto LB agar containing 100 mg/L of bromoxynil octanoate and 100 mg/L of ampicillin and were incubated at 37 °C for 16 h. A positive clone that produced clear transparent halos was picked out and tested by HPLC analysis for its ability to degrade bromoxynil octanoate.

The DNA fragment inserted into that positive clone was sequenced by Shanghai Invitrogen Biotechnology Co., Ltd. The sequence was analyzed by a SignalP 4.0 server to identify the signal peptide.<sup>15</sup> A sequence similarity comparison was performed with the Blast 2.0 program.<sup>16</sup> The amino acid sequences of BroH and its most closely related proteins in GenBank were aligned with the BioEdit 6.0 software, and a phylogenetic tree was constructed using the neighbor-joining method with 1000 bootstrap replicates in the Molecular Evolutionary Genetics Analysis software (MEGA version 4.0).<sup>12</sup>

**Esterase Gene Expression and Purification of the Recombinant Esterase.** The gene coding for the esterase BroH without its translation stop codon was amplified by PCR with the following primer pairs: 5'-gtggatccatgggagacggcatgac-3'/5'-gtgctcgagagccgaccatcgcg-3' (restriction enzyme digestion sites are in italics). The resulting PCR product was then inserted into pET29a (+), which had been digested with *Bam*HI and *Xho*I. The recombinant plasmid pET-BroH was then transformed into *E. coli* BL21 (DE3). Transformed cells were picked and grown in 3 mL of LB supplemented with 50 mg/L of kanamycin at 37 °C for 12 h. Next, the cells were inoculated at 1% (v/v) into 100 mL of fresh LB containing 50 mg/L of kanamycin and incubated at 37 °C. When cell growth reached the midlog phase ( $\text{OD}_{600\text{ nm}} = 0.6$ ), isopropyl- $\beta$ -D-thiogalactopyranoside (IPTG) was added to the medium at a final concentration of 1 mM to induce the target protein, and the cells were incubated for an additional 4 h at 30 °C. The cells were then harvested, resuspended in 10 mL binding buffer (20 mM  $\text{Na}_3\text{PO}_4$ , 500 mM  $\text{NaCl}$ , pH 7.8), and sonicated. The suspension was centrifuged at 12000g for 15 min at 4 °C. The supernatant was applied to a Ni-NTA affinity chromatography column (Qiagen), and the protein was eluted with washing buffer (20 mM  $\text{Na}_3\text{PO}_4$ , 500 mM  $\text{NaCl}$ , pH 6.0) containing an increasing concentration of imidazole (10, 50, 75, 100, 150, and 200 mM).<sup>14</sup> The target protein was eluted at 150–200 mM imidazole. The protein concentration was quantified by the Bradford method with bovine serum albumin (BSA) as a standard. The recombinant protein was dialyzed in phosphate-buffered saline (PBS; 8.0 g of  $\text{NaCl}$ , 0.2 g of  $\text{KCl}$ , 1.44 g of  $\text{Na}_2\text{HPO}_4$ , and 0.24 g of  $\text{KH}_2\text{PO}_4$

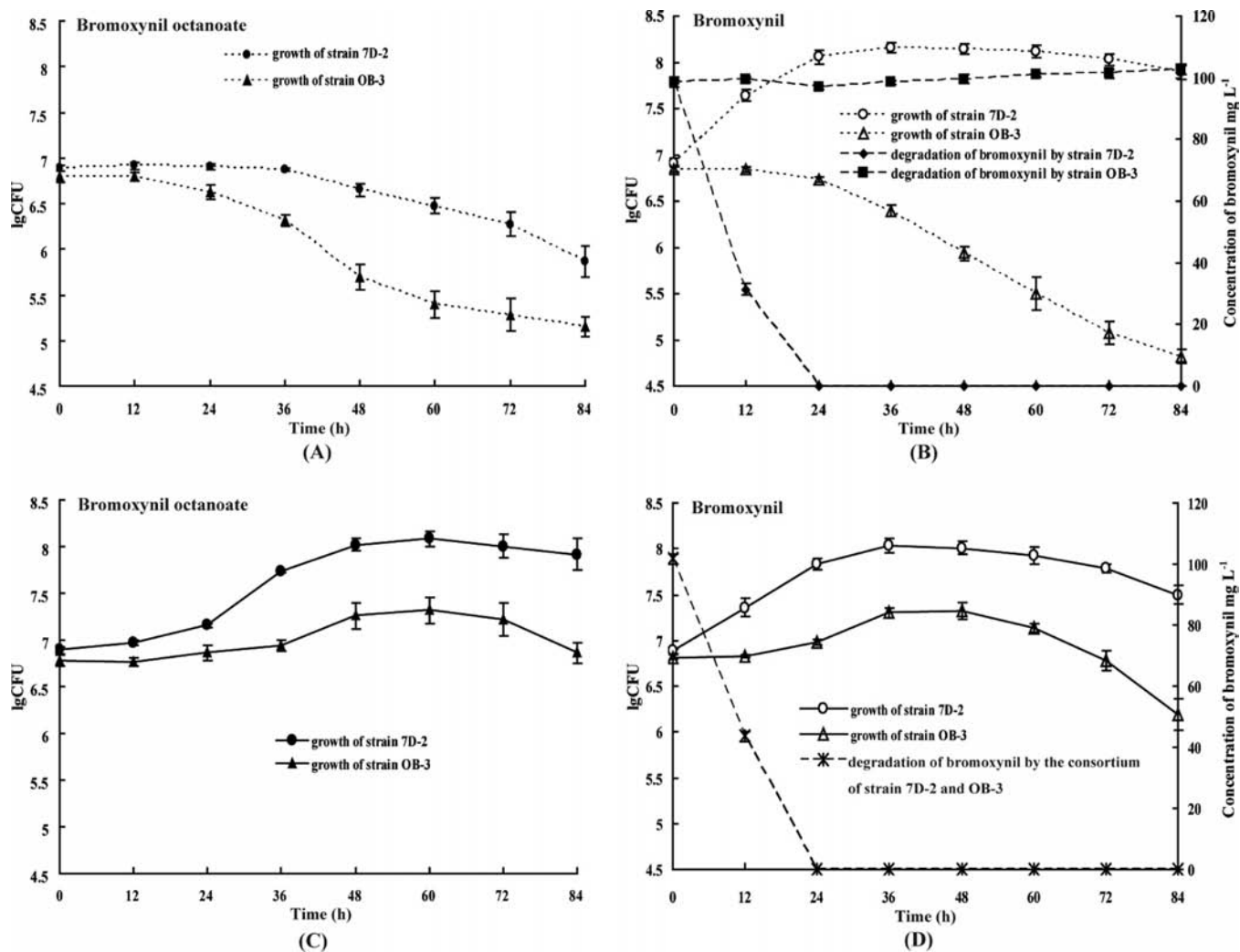


**Figure 1.** Growth rate and degradation of bromoxynil octanoate and bromoxynil by strains OB-3 and 7D-2: (A) the ability of strain OB-3 and strain 7D-2 to grow when inoculated separately in MMBO; (B) the rate of degradation of bromoxynil and the growth of each strain when inoculated separately in MMB; (C) synergistic growth of strains OB-3 and 7D-2 when inoculated in a consortium in MMBO; (D) rate of synergistic degradation of bromoxynil and the growth of strains OB-3 and 7D-2 when inoculated in a consortium in MMB.

per liter of water at pH 7.4) overnight to remove the imidazole and the Ni<sup>2+</sup>. The purified BroH protein was analyzed by sodium dodecyl sulfate polyacrylamide gel electrophoresis (SDS-PAGE) with a 12% polyacrylamide resolving gel and a 5% stacking gel, which was subsequently stained with Coomassie brilliant blue G250 (Amresco, USA).

**Characteristics of the Esterase BroH.** A standard enzyme assay was performed according to the method previously described by Nie et al.<sup>17</sup> with some modifications. Briefly, 5  $\mu$ L of purified esterase was added to 3 mL of PBS with 100 mg/L of bromoxynil octanoate and incubated at 37 °C for 5 min. The reaction was stopped by the addition of 100  $\mu$ L of HCl (5 M).

The optimum temperature for BroH activity was determined by measuring its hydrolytic activity toward bromoxynil octanoate at various temperatures (10–70 °C). To determine its thermal stability, the enzyme was preincubated in PBS (pH 7.4) at different temperatures for 30 min, and the residual activity was subsequently tested. Enzymatic activity was measured under standard conditions.

The optimum pH range of BroH activity was determined by incubating the enzyme with bromoxynil octanoate for 5 min at 37 °C at pH values from 3.5 to 10.5. The following buffers were used:<sup>18</sup> 100 mM citric acid–sodium citrate buffer (pH 3.5–6), 50 mM phosphate buffer (pH 5.5–8), 50 mM Tris–HCl buffer (pH 7.5–9), and 20 mM glycine–NaOH buffer (pH 8.5–10.5). Enzyme activity was then measured under standard conditions.

The effect of different metal ions, detergents, and inhibitors on the enzymatic activity of BroH was assessed in PBS (pH 7.4) at 37 °C. Metal ions (CaCl<sub>2</sub>, FeCl<sub>2</sub>, FeCl<sub>3</sub>, AlCl<sub>3</sub>, LiCl, ZnCl<sub>2</sub>, MgCl<sub>2</sub>, CoCl<sub>2</sub>, CdCl<sub>2</sub>, CrCl<sub>3</sub>, CuCl<sub>2</sub>, AgNO<sub>3</sub> (in water instead of PBS), HgCl<sub>2</sub>, MnCl<sub>2</sub> and NiSO<sub>4</sub>) were added at a final concentration of 1 mM, while detergents (SDS, Triton X-100, Tween-20, and Tween-80) were used at a final concentration of 0.5%, and inhibitors (phenylmethanesulfonyl fluoride (PMSF), ethylenediaminetetraacetic acid (EDTA), diethyl pyrocarbonate (DEPC), iodoacetamide, and 1,10-phenanthroline) were used at a final concentration of 1 mM.

The enzymatic activity of BroH toward *p*-nitrophenyl esters with different chain lengths and various pesticides with carboxylic acid esters was also evaluated according to the method previously described by Shabtai et al.<sup>19</sup> The kinetic activity of BroH acting on different substrates was obtained from a Lineweaver–Burk plot against different substrate concentrations in PBS (pH 7.4) at 37 °C. In all cases, no more than 10% of the substrate was hydrolyzed.

**Nucleotide Sequence Accession Number.** The nucleotide sequence of the esterase gene *broH* from *Sphingopyxis* sp. OB-3 was deposited in the GenBank database under accession number JN831942.

## RESULTS

**Characterization of the Two Bacterial Strains in the Bromoxynil Octanoate Degrading Consortium.** The

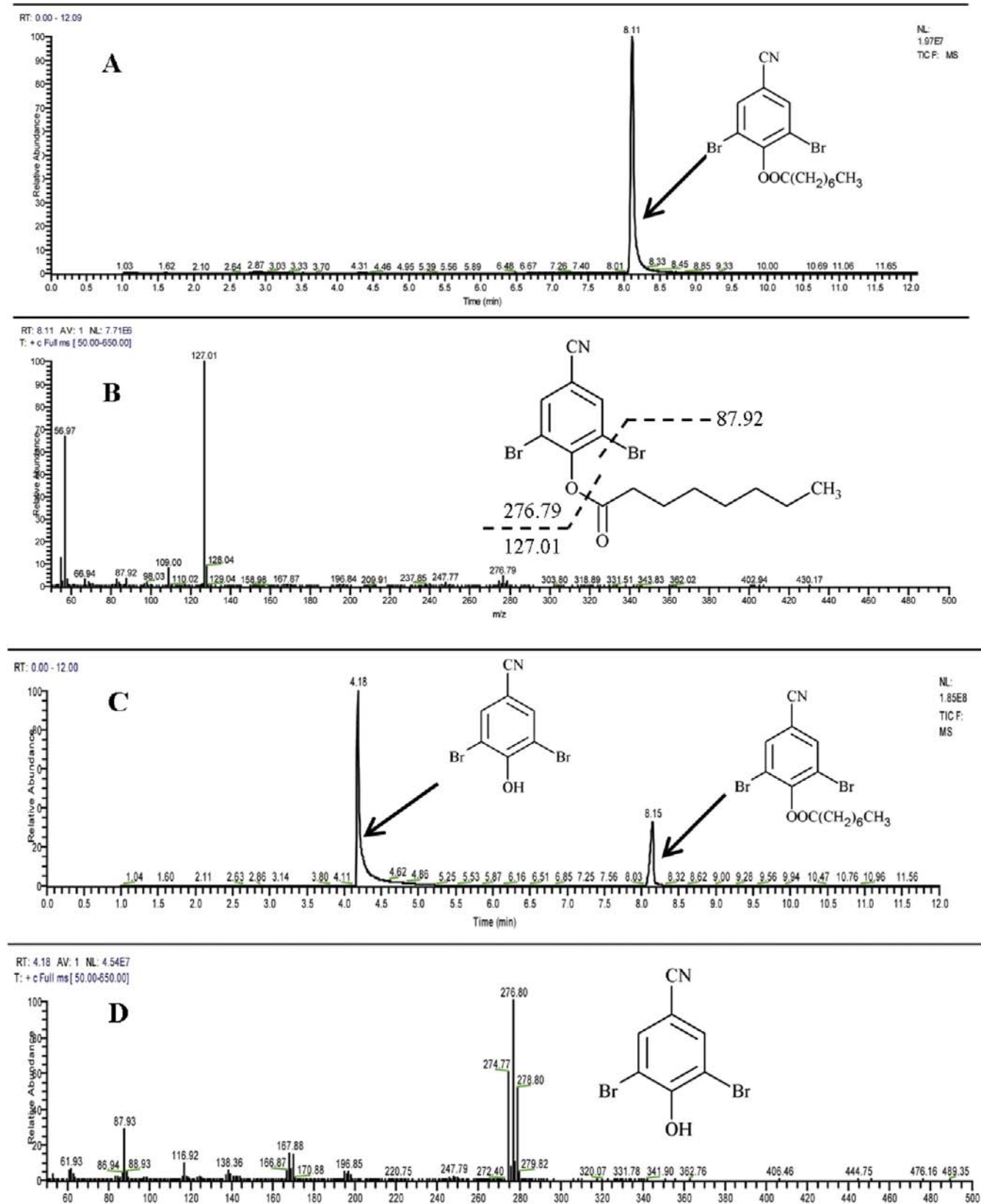


**Figure 2.** GC-MS profiles for bromoxynil octanoate and its metabolite produced by strain OB-3: (A, B) GC chromatogram and MS spectrum of bromoxynil octanoate, respectively; (C, D) GC chromatogram and MS spectrum of the metabolite bromoxynil, respectively.

original single colony that grew on the MMBO agar was found to be capable of mineralizing bromoxynil octanoate. After several streakings on LB agar over the course of 60 h, another small, light

yellow, and convex colony (corresponding to strain OB-3) appeared in the original colorless and flat colony (corresponding to strain 7D-2). In the end, two different bacterial strains were

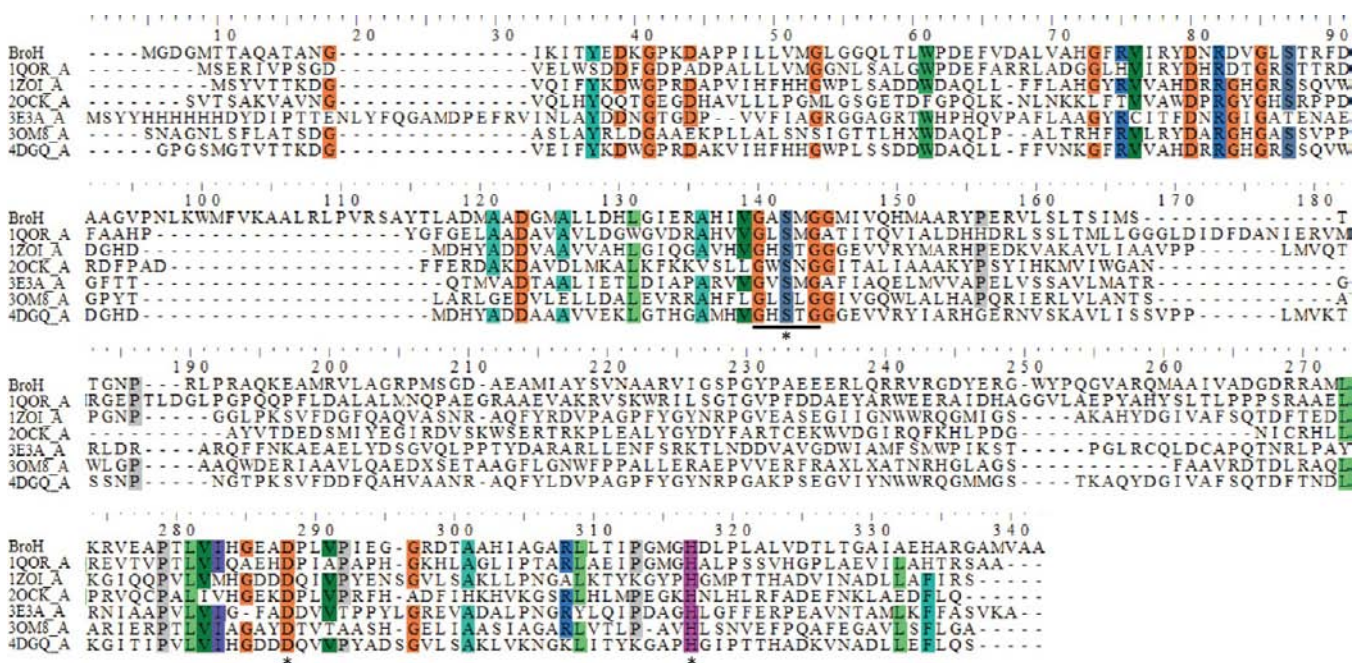


**Figure 3.** Sequence alignment of BroH with the most closely related proteins available in the Protein Data Bank (PDB): 1Q0R\_A, an acylinomyacin methyltransferase (Rdmc) from *Streptomyces purpurascens*; 3OM8\_A, a hydrolase from *Pseudomonas aeruginosa* Pa01; 1Z0I\_A, a stereoselective esterase from *Pseudomonas putida* lfo 12996; 3E3A\_A, an  $\alpha/\beta$ -hydrolase fold of Rv0554 from *Mycobacterium tuberculosis*; 4DQ0\_A, an  $\alpha/\beta$ -hydrolase fold from *Burkholderia cenocepacia*. The conserved motif (GXSG) is underlined, and the amino acids that form the catalytic triad (Ser124, Asp251 and His279) are indicated by asterisks.

purified from these two colonies. Strain OB-3 and strain 7D-2 are both Gram-negative, rod-shaped, and motile aerobes. Strain OB-3 is approximately 1.2–1.5  $\mu\text{m}$  in length and 0.5–0.7  $\mu\text{m}$  in width, while strain 7D-2 is slightly longer (approximately 1.3–1.7  $\mu\text{m}$  in length and 0.5–0.7  $\mu\text{m}$  in width). Strain OB-3 was determined to be related to the *Sphingopyxis* species lineage and was closely clustered with *S. taejonensis* JSS54<sup>T</sup> and *S. granuli* Kw07<sup>T</sup>, with sequence similarity scores of 98.7% and 98.6%, respectively. Strain 7D-2 was related to the *Comamonas* species lineage and was closely clustered with *C. testosteroni* ATCC 11996<sup>T</sup> and *C. thiooxydans* S23<sup>T</sup>, with sequence similarity scores of 99.8% and 99.79%, respectively. On the basis of the above phenotypic characteristics and phylogenetic analyses, strains OB-3 and 7D-2 were identified as *Sphingopyxis* species and *Comamonas* species, respectively.

**Synergistic Degradation and Growth of the Consortium.** When strain OB-3 was inoculated alone, it was able to degrade approximately 20% of the supplied 100 mg/L of bromoxynil octanoate in MMBO over the course of 84 h. Because of its lower solubility and heterogeneity in the medium, the concentration of bromoxynil octanoate was not determined at any interval before the final 84 h. The number of OB-3 cells decreased from  $6.2 \times 10^6$  CFU/mL to  $1.5 \times 10^5$  CFU/mL, which suggests that strain OB-3 could not use bromoxynil octanoate as its sole carbon source for growth (Figure 1A). In MMB medium, the concentration of bromoxynil remained unchanged, and the number of OB-3 cells decreased sharply, which suggested that strain OB-3 could not degrade bromoxynil (Figure 1B).

When strain 7D-2 was inoculated alone, it was able to completely degrade 100 mg/L bromoxynil in MMB medium in 24 h (Figure 1B). The number of 7D-2 cells increased to  $1.5 \times 10^8$  CFU/mL in 36 h, remained stable for 12 h, and then decreased slightly, which suggests that strain 7D-2 could use bromoxynil as its sole carbon source (Figure 1B). When the

strain was grown in MMBO, the concentration of bromoxynil octanoate remained unchanged, and the number of 7D-2 cells decreased from  $7.8 \times 10^6$  CFU/mL to  $7.7 \times 10^5$  CFU/mL, which suggested that strain 7D-2 could not degrade bromoxynil octanoate (Figure 1A).

When strains OB-3 and 7D-2 were inoculated as a consortium, the bromoxynil octanoate present in MMBO was completely degraded. After a lag phase of 24 h, the number of cells of strain OB-3 increased to its peak of  $2.1 \times 10^7$  CFU/mL by 60 h and then declined slowly (Figure 1C). For strain 7D-2, the lag phase lasted for only 12 h, and then the number of cells increased to its peak of  $1.2 \times 10^8$  CFU/mL at 60 h (Figure 1C). When both strains were grown together in MMB, bromoxynil was completely degraded in 84 h, and strain 7D-2 grew at a similar rate as when it was inoculated alone with a slightly smaller biomass (Figure 1D). Interestingly, strain OB-3 began to increase its numbers at 12 h and reached its peak of  $2.1 \times 10^7$  CFU/mL at 36 h. However, the growth rate of strain OB-3 began to decline at 48 h (Figure 1D).

The growth of these two strains appeared to be syntrophic, because strain OB-3 could not degrade bromoxynil independently, while strain 7D-2 was unable to degrade bromoxynil octanoate independently. A single inoculation with each isolate could not utilize bromoxynil octanoate to grow, while an inoculation with the consortium permitted both strains to grow and resulted in the mineralization of bromoxynil octanoate due to cooperative biodegradation by the two strains. Strain OB-3 converted bromoxynil octanoate to bromoxynil, which allowed strain 7D-2 to utilize bromoxynil as its sole carbon source for growth. This in turn facilitated the growth of strain OB-3 by providing it with a carbon source as well. These results also suggest strain OB-3 expresses an esterase that is responsible for converting bromoxynil octanoate to bromoxynil and is therefore

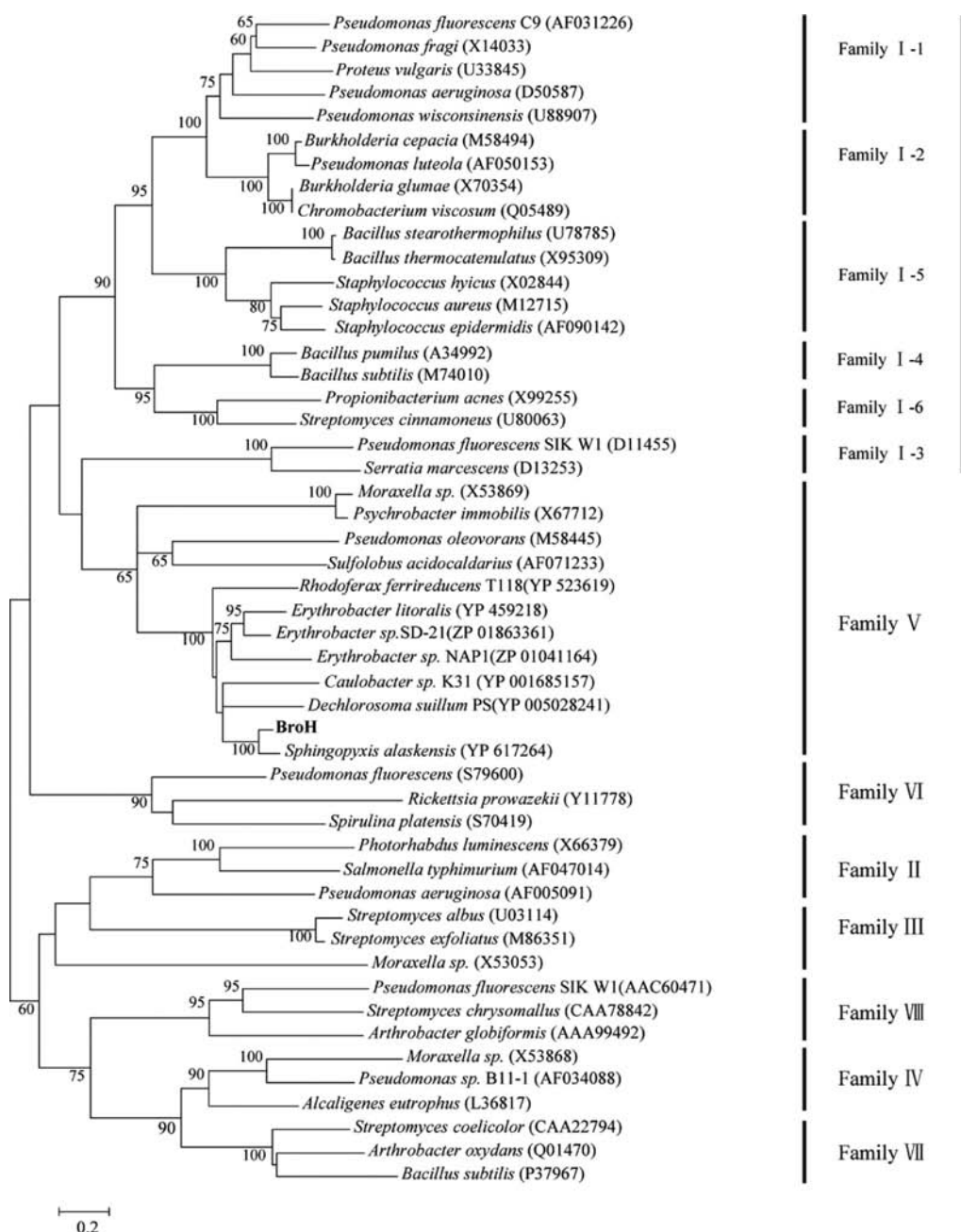


**Figure 4.** Phylogenetic analysis of BroH, revealing its relation to other esterases and lipases from subfamilies I–VIII. The phylogenetic tree was constructed by the neighbor-joining method with 1000 bootstrap replicates (values >60% are shown at the nodes). The related protein sequences retrieved from GenBank were aligned using ClustalW. Bar, 0.2.

necessary for the mineralization of bromoxynil octanoate by the consortium.

**Identification of Bromoxynil Production in Strain OB-3 by GC-MS.** To further confirm that bromoxynil octanoate is converted to bromoxynil by strain OB-3, the metabolite produced during bromoxynil octanoate degradation in strain OB-3 was detected and identified by GC-MS (Figure 2). The retention time of bromoxynil octanoate was 8.11 min (Figure 2A), and its MS spectrum is shown in Figure 2B. In contrast, the retention time of the metabolite was 4.18 min (Figure 2C). On the basis of the mass spectra data and an identification program that utilizes the NIST library, the metabolite produced by strain OB-3 could be identified as bromoxynil (Figure 2D).

### Cloning and Sequence Analysis of the Bromoxynil Octanoate Hydrolyzing Esterase Gene.

To clone the esterase gene that is responsible for transforming bromoxynil octanoate to bromoxynil in strain OB-3, a shotgun cloning method was used. A positive clone that produced a transparent halo around the colony was selected from approximately 8000 transformants, and the fragment inserted in this positive clone was sequenced. This fragment was 2179 bp long and contained four complete ORFs. These ORFs were each subcloned into the pMD18-T vector and then transformed into competent *E. coli* DH5 $\alpha$  cells. One ORF, designed *broH*, was confirmed to be the gene that encoded the bromoxynil octanoate ester bond-hydrolyzing protein. This ORF consists of 915 bp that encode 304 amino acids. No signal peptide region was found at the N-

terminal region of *broH*. The encoded protein, BroH, shows 27–34% similarity with other functionally confirmed esterases and hydrolase fold proteins for which crystal structures have been elaborated: e.g., the aclacinomycin methylesterase (Rdmc) (1QOR\_A) from *Streptomyces purpurascens* (34% similarity), a hydrolase (3OM8\_A) from *Pseudomonas aeruginosa* Pa01 (34% similarity), a stereoselective esterase (1ZOI\_A) from *Pseudomonas putida* lfo 12996 (28% similarity), an  $\alpha/\beta$ -hydrolase fold of Rv0554 (3E3A\_A) from *Mycobacterium tuberculosis* (29% similarity), and an  $\alpha/\beta$ -hydrolase fold (4DGQ\_A) from *Burkholderia cenocepacia* (27% similarity). Sequence alignment of BroH with these hydrolase proteins demonstrated that BroH contains the same Ser-His-Asp/Glu catalytic triad (Ser124, Asp251 and His279) as  $\alpha/\beta$ -hydrolase fold proteins and also contains the feature signature GX SXG (residues 122–126) (Figure 3).<sup>20,21</sup>

On the basis of the phylogenetic analysis of BroH that reveals its relation to other esterases and lipases from subfamilies I to VIII (Figure 4), BroH was found to be clustered with the subfamily V esterases, which contain a catalytic triad that is typical of  $\alpha/\beta$ -hydrolase fold proteins. On the basis of the amino acid sequence comparison (Figure 3) and phylogenetic analysis (Figure 4), BroH most likely belongs to subfamily V of bacterial lipolytic enzymes.

**Gene Expression and Purification of the Recombinant Esterase BroH.** Recombinant BroH was expressed in *E. coli* BL21 (DE3) and purified from the supernatant of cell lysates using Ni-nitrilotriacetic acid affinity chromatography. The recombinant BroH was primarily eluted when the elution buffer contained 150–200 mM imidazole. The molecular mass of the denatured BroH was found to be approximately 33 kDa, as determined by SDS-PAGE (Figure 5), which corresponds to the predicted molecular mass (32521 Da).

**Characterization of the BroH Esterase.** The optimal temperature for BroH activity was determined to be 35 °C, and a thermostability analysis indicated that BroH is extremely

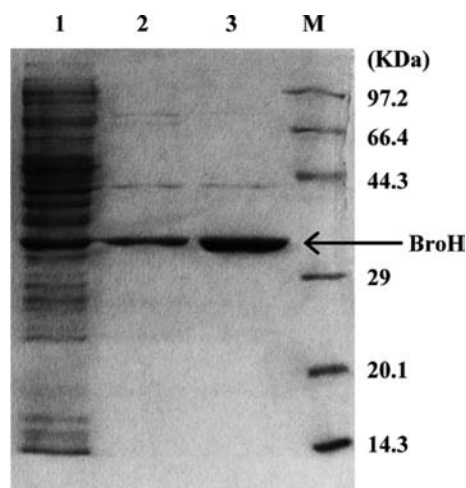


**Figure 5.** Expression and purification of recombinant BroH: lane M, protein molecular weight marker (TaKaRa); lane 1, the supernatant from a cell lysate from the induced *E. coli* BL21 (DE3) containing pET-BroH; lane 2, BroH purified from a Ni-NTA column and eluted by buffer containing 150 mM imidazole; lane 3, BroH purified from a Ni-NTA column and eluted by buffer containing 200 mM imidazole. Proteins obtained at various purification steps were separated by 12% SDS-PAGE. The gel was stained by Coomassie brilliant blue G250.

sensitive to temperatures over 35 °C (Figure 6A). The optimal pH for BroH activity was determined to be 7.5 with a greater than 60% relative activity between pH 6.5–8 (Figure 6B). BroH was strongly inhibited by 1 mM of  $\text{Al}^{3+}$ ,  $\text{Ni}^{2+}$ , and  $\text{Hg}^{2+}$  but only slightly inhibited by 1 mM of  $\text{Cd}^{2+}$ ,  $\text{Cr}^{3+}$ ,  $\text{Zn}^{2+}$ ,  $\text{Li}^+$ ,  $\text{Ag}^+$ , and  $\text{Fe}^{3+}$  (Figure 7). The surfactants Triton X-100, Tween-20, and Tween-80 inhibited approximately 50% of the total BroH activity, while SDS almost completely inhibited its activity. The serine inhibitor PMSF along with both the histidine modifier DEPC and iodoacetamide significantly inhibited the enzymatic activity of BroH (Table 1), while the chelating agent 1,10-phenanthroline had no significant effect.

To investigate the substrate specificity of BroH, its kinetic parameters were examined when provided with various substrates (Table 2). BroH showed the highest activity toward *p*-nitrophenyl caproate (C6), as determined by the catalytic efficiency value ( $V_{\text{max}}/K_m$ ), and the activity decreased when the aliphatic length of the substrate increased. Almost no hydrolytic activity was observed toward *p*-nitrophenyl palmitate (C16). The structures of *p*-nitrophenyl octanoate (C8) and bromoxynil octanoate were similar, but the hydrolytic activity of BroH on *p*-nitrophenyl octanoate was 6.5-fold higher than that of bromoxynil octanoate. BroH was also able to hydrolyze some pesticides with carboxylic acid esters, such as fenoxaprop-P-ethyl, cyhalofop-butyl, clodinafop-propargyl, and quizalofop-P (data not shown).

## DISCUSSION

The extensive use of brominated cyanophenyl herbicides, specifically bromoxynil octanoate and bromoxynil, has also caused environmental pollution and ecosystem damage.<sup>4</sup> Microbially mediated degradation is thought to be a major avenue of dissipating bromoxynil octanoate and bromoxynil from the environment. Although several bromoxynil-degrading strains have previously been isolated,<sup>1,8</sup> *Acinetobacter* sp. XB2 is the only bromoxynil octanoate degrading pure culture that has been reported.<sup>7</sup> In this study, a natural consortium composed of two bacterial strains was found to be capable of transforming bromoxynil octanoate to bromoxynil, which was then mineralized. This represents the first report of the mineralization of bromoxynil octanoate by a bacterial consortium.

The consortium contained two strains that were identified as *Sphingopyxis* sp. OB-3 and *Comamonas* sp. 7D-2. The genus *Sphingopyxis* was created by Takeuchi et al.<sup>22</sup> from the genus *Sphingomonas*, which was famous for its metabolic capacity. The *Sphingopyxis* species has been reported to be capable of degrading the xenobiotic chlorophenol.<sup>23</sup> *Comamonas* species are quite ubiquitous in the environment and have been noted for their capability to degrade aromatic compounds<sup>9,24–27</sup> and their involvement in the synergistic degradation of pollutants.<sup>28–30</sup> In this study, a *Sphingopyxis* species and a *Comamonas* species formed a consortium that was capable of mineralizing a brominated cyanophenyl herbicide.

During the initial isolation of this bromoxynil octanoate degrading consortium, only colorless, flat colonies appeared on agar plates, while the light yellow colonies appeared within the earlier colonies only after 60 h. This result suggests that the first strain (7D-2) is more competitive than the second (OB-3). *Comamonas* species members are known for their fast growth on agar plates; therefore, they most likely overgrew strain OB-3 initially. This is consistent with the number of cells observed for each strain during the synergistic degradation and growth experiments (Figure 1). In contrast, the close contact of these

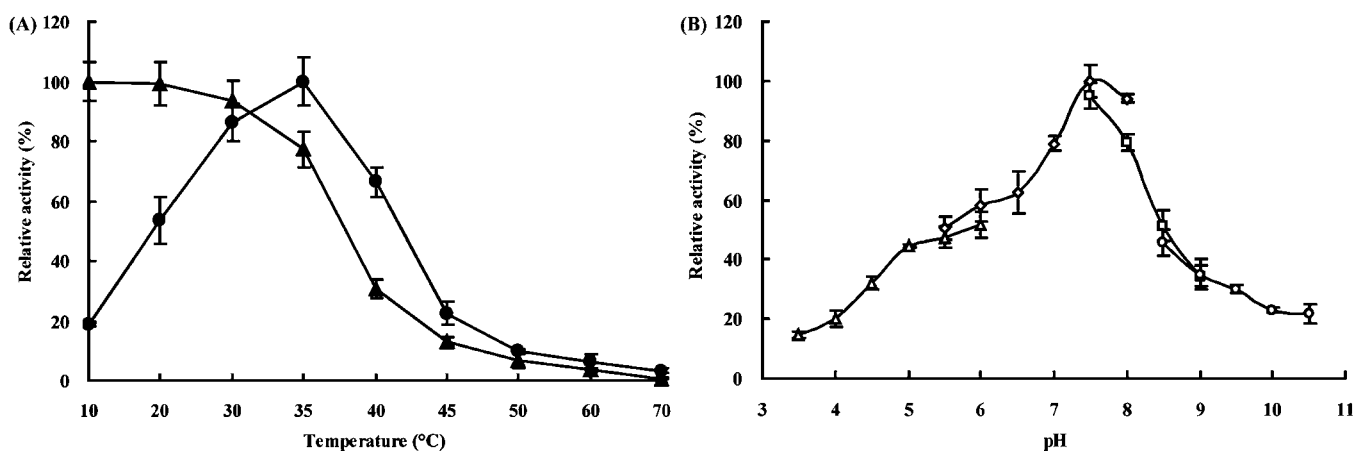


**Figure 6.** (A) Effect of temperature on the activity and stability of BroH: (●) the relative activity of purified BroH assayed at each temperature; (▲) the effect of temperature on BroH stability determined by incubating the enzyme at each temperature for 30 min and then assaying the residual activity. (B) Effect of pH on the activity of BroH. Relative activity assays were conducted at 37 °C in 100 mM citric acid–sodium citrate buffer (pH 3.5–6; △), 50 mM phosphate buffer (pH 5.5–8; ◇), 50 mM Tris–HCl buffer (pH 7.5–9; □), or 20 mM glycine–NaOH buffer (pH 8.5–10.5; ○).

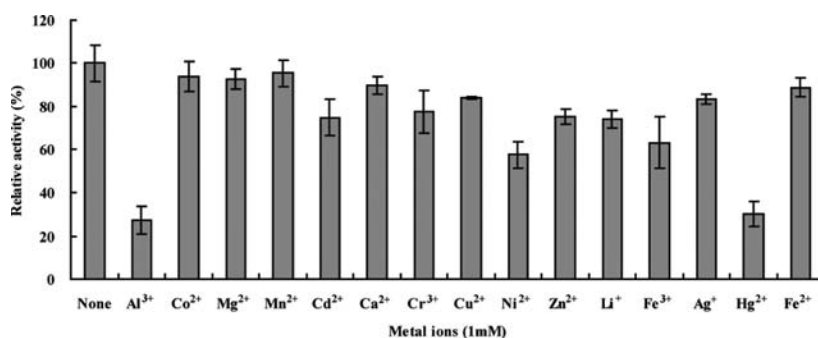


**Figure 7.** Effect of various metal ions on BroH activity. Relative activity assays were performed at 37 °C in PBS (pH 7.4) containing 1 mM of various metal ions, with the exception of AgNO<sub>3</sub>, which required water instead of PBS.

**Table 1.** Effect of Various Detergents and Inhibitors on BroH Activity

detergent or inhibitor	rel activity (%)	detergent or inhibitor	rel activity (%)
none	100 ± 4.8	SDS	9.5 ± 1.2
EDTA	111.4 ± 2.8	Tween-20	51.1 ± 3.6
1,10-phenanthroline	99.4 ± 2.6	Tween-80	57.7 ± 6.8
iodoacetamide	37.7 ± 2.8	PMSF	23.0 ± 3.0
Triton X-100	43.2 ± 2.6	DEPC	22.2 ± 4.8

two colonies suggests that they are closely related in nature and interact in a synergistic manner.

The synergistic metabolism in which a bacterial consortium degrades organic pollutants is an interesting phenomenon that is widespread in nature.<sup>31</sup> Various bacterial consortia have been isolated and reported to synergistically degrade or even mineralize different xenobiotics, such as dicamba,<sup>32</sup> *o*-methoxybenzoate,<sup>33</sup>  $\alpha$ -hexachlorocyclohexane,<sup>34</sup> fluorobenzene,<sup>35</sup> linuron,<sup>28</sup> 4-chloroaniline,<sup>29</sup> and atrazine.<sup>30</sup> This synergistic degradation can occur through two mechanisms: (i) complementation of metabolic deficiencies, in which the degrading bacteria are fastidious and depend on other strains that provide essential growth factors or nutrients,<sup>36</sup> or (ii) associated metabolism, in which cross-feeding with metabolites from the degradation pathway occurs between members of the consortium. For example, in a four-member atrazine-degrading consortium, *Clavibacter michiganense* ATZ1 initiates the degradation of the

**Table 2.** Kinetic Parameters of BroH Activity on Various Substrates

substrate	$K_m$ ( $\mu$ M)	$V_{max}$ ( $\mu$ M/(min mg))	$V_{max}/K_m$ (1/(min mg))
<i>p</i> -nitrophenyl acetate (C2) <sup>a</sup>			
<i>p</i> -nitrophenyl butyrate (C4)	252.7	133491.1	528.3
<i>p</i> -nitrophenyl caproate (C6)	135	119289.9	883.6
<i>p</i> -nitrophenyl octanoate (C8)	25.7	10701.5	416.4
<i>p</i> -nitrophenyl caprate (C10)	27.7	10970.4	396.0
<i>p</i> -nitrophenyl laurate (C12)	31.4	5627.2	179.2
<i>p</i> -nitrophenyl myristate (C14) <sup>a</sup>			
bromoxynil octanoate	740	31297.3	42.3

<sup>a</sup>Because *p*-nitrophenyl acetate was self-hydrolyzed in water and hydrolysis of *p*-nitrophenyl myristate by BroH occurred so slowly, the kinetic parameters were not calculated. However, BroH was able to transform these two *p*-nitrophenyl esters.

*s*-triazine herbicide by removing the side chain, which allows the *Pseudomonas* sp. strain CN1 to subsequently cleave the ring.<sup>37</sup>

Our results suggest that the second mechanism, associated metabolism, is utilized by our consortium in the synergistic degradation of bromoxynil octanoate. *Comamonas* sp. 7D-2,



which could not degrade bromoxynil octanoate independently, formed colonies in MMB and used bromoxynil octanoate for growth in the presence of strain OB-3, which suggests that strain OB-3 transformed bromoxynil octanoate into a substrate that could be used by strain 7D-2. Because both strains could grow when bromoxynil octanoate was the sole carbon source, it is likely that strain 7D-2 can in turn provide strain OB-3 with a usable carbon source by metabolizing bromoxynil. Therefore, these two strains each require compounds that only the other can provide, which reveals the presence of a syntrophic relationship between the two. Furthermore, a mutualistic effort of both OB-3 and 7D-2 is required for the mineralization of bromoxynil octanoate, and their synergistic interaction within the consortium stimulates the degradation of both bromoxynil octanoate and bromoxynil.

Lipases (carboxylesterases, EC 3.1.1.3) and esterases (EC 3.1.1.1) have previously been identified as efficient biocatalysts for biotransformations. Because of their availability and their ability to catalyze a wide range of reactions, microbial lipases and esterases have been the subject of many important studies.<sup>38</sup> Esterases and lipases found in bacteria were divided into eight subfamilies (from I to VIII) by Arpigny and Jaeger.<sup>38</sup> The esterase BroH that was cloned from strain OB-3 is not only responsible for converting bromoxynil octanoate to bromoxynil but is also required for the mineralization of bromoxynil octanoate by the consortium; therefore, it links strains OB-3 and 7D-2. BroH belongs to the  $\alpha/\beta$ -hydrolase fold protein family and contains both the catalytic center Ser-His-Asp/Glu and the highly conserved pentapeptide GX SXG that is characteristic of  $\alpha/\beta$ -hydrolase fold proteins. The substrate spectrum of BroH was found to be broad. It was able to hydrolyze many chemicals that contained carboxylic acid esters, such as *p*-nitrophenyl esters (C2–C14). BroH could also hydrolyze other pesticide esters, such as fenoxaprop-*p*-ethyl, cyhalofop-butyl, fluazifop-*p*-butyl, clodinafop-propargyl, and quizalofop-*p*. However, it was not able to hydrolyze pyrethroids, such as cypermethrin, bifenthrin, cyhalothrin, and deltamethrin (data not shown). The catalytic efficiency value ( $V_{\max}/K_m$ ) demonstrated that *p*-nitrophenyl caproate (C6) was the most efficient catalytic substrate. A specificity profile classified the enzyme as an esterase because maximal activity was observed on the short-chain fatty acid esters *p*-nitrophenyl caproate and octanoate (C6–C8), while activity on long-chain insoluble esters was low. This classification corresponded with the phylogenetic analysis, which suggested that BroH is clustered with esterases in subfamily V. Specifically, the ability of PMSF to inhibit BroH suggests that BroH belongs to the serine hydrolase family. The 6.5-fold lower activity of BroH on bromoxynil octanoate in comparison to *p*-nitrophenyl octanoate (C8) may be due the stereochemical hindrance of the two bromine atoms on the 3- and 5-sites of bromoxynil octanoate.

The esterase BroH is essential for the mineralization of bromoxynil octanoate by the bacterial consortium described here. However, the physiological role of BroH in strain OB-3 remains unclear. The effect of knocking out the *broH* gene on the degradation of bromoxynil octanoate and the growth of the consortium is also unknown.

## AUTHOR INFORMATION

### Corresponding Author

\*J.-D.J.: e-mail, jiang\_jjd@njau.edu.cn; tel, (+86)2584396348; fax, (+86)2584396314.

## Funding

This work was supported by grants from the National Science and Technology Support Plan (2013AA102804), the Chinese National Science Foundation for Excellent Young Scholars (31222003), the Chinese National Natural Science Foundation (31070100), the Program for New Century Excellent Talents in University (NCET-12-0892), and the Outstanding Youth Foundation of Jiangsu Province (BK20130029).

## Notes

The authors declare no competing financial interest.

## REFERENCES

- (1) Veselá, A.; Franc, M.; Pelantová, H.; Kubá, D.; Vejvoda, V.; Šulc, M.; Bhalla, T.; Macková, M.; Lovecká, P.; Jan, P. Hydrolysis of benzonitrile herbicides by soil actinobacteria and metabolite toxicity. *Biodegradation* **2010**, *21*, 761–770.
- (2) Roberts, T. R.; Hutson, D. H.; Lee, P. W.; Nicholls, P. H.; Plimmer, J. R. *Metabolic pathways of agrochemicals*; The Royal Society of Chemistry: Cambridge, United Kingdom, 1998; Part 1, Herbicides and plant growth regulators.
- (3) Miller, J. J.; Hill, B. D.; Chang, C.; Lindwall, C. W. Residue detections in soil and shallow groundwater after long-term herbicide applications in southern Alberta. *Can. J. Soil. Sci.* **1995**, *75*, 349–356.
- (4) Semchuk, K. M.; McDuffie, H. H.; Senthilselvan, A.; Dosman, J. A.; Cessna, A. J.; Irvine, D. G. Factors associated with detection of bromoxynil in a sample of rural residents. *J. Toxicol. Environ. Health A* **2003**, *66*, 103–132.
- (5) Ma, J.; Wang, P.; Chen, J.; Sun, Y.; Che, J. Differential response of green algal species *Pseudokirchneriella subcapitata*, *Scenedesmus quadricauda*, *Scenedesmus obliquus*, *Chlorella vulgaris* and *Chlorella pyrenoidosa* to six pesticides. *Pol. J. Environ. Stud.* **2007**, *16*, 847–851.
- (6) Buckland, J. L.; Collins, R. F.; Puiiin, E. M. Metabolism of bromoxynil octanoate in growing wheat. *Pestic. Sci.* **1973**, *4*, 149–162.
- (7) Cai, T.; Chen, L.; Xu, J.; Cai, S. Degradation of bromoxynil octanoate by strain *Acinetobacter* sp. XB2 isolated from contaminated soil. *Curr. Microbiol.* **2011**, *63*, 218–225.
- (8) McBride, K. E.; Kenny, J. W.; Stalker, D. M. Metabolism of the herbicide bromoxynil by *Klebsiella pneumoniae* subsp. *ozaenae*. *Appl. Environ. Microbiol.* **1986**, *52*, 325–330.
- (9) Chen, K.; Huang, L. L.; Xu, C. F.; Liu, X. M.; He, J.; Zinder, S. H.; Li, S. P.; Jiang, J. D. Molecular characterisation of the enzymes involved in the degradation of a brominated aromatic herbicide. *Mol. Microbiol.* **2013**, *89*, 1121–1139.
- (10) Li, R.; Zheng, J.; Wang, R.; Song, Y.; Chen, Q.; Yang, X.; Li, S.; Jiang, J. Biochemical degradation pathway of dimethoate by *Paracoccus* sp. Lgij-3 isolated from treatment wastewater. *Int. Biodeter. Biodegr.* **2010**, *64*, 51–57.
- (11) Thompson, J. D.; Gibson, T. J.; Plewniak, F.; Jeanmougin, F.; Higgins, D. G. The CLUSTAL\_X windows interface: flexible strategies for multiple sequence alignment aided by quality analysis tools. *Nucleic Acids Res.* **1997**, *25*, 4876–4882.
- (12) Kumar, S.; Nei, M.; Dudley, J.; Tamura, K. MEGA: a biologist-centric software for evolutionary analysis of DNA and protein sequences. *Briefings Bioinf.* **2008**, *9*, 299–306.
- (13) Sambrook, J.; Russell, D. W. *Molecular cloning: a laboratory manual*, 3rd ed.; Cold Spring Harbor Laboratory Press: Cold Spring Harbor, NY, 2001.
- (14) Wang, G.; Li, R.; Li, S.; Jiang, J. A novel hydrolytic dehalogenase for the chlorinated aromatic compound chlorothalonil. *J. Bacteriol.* **2010**, *192*, 2737–2745.
- (15) Petersen, T. N.; Brunak, S.; von Heijne, G.; Nielsen, H. SignalP 4.0: discriminating signal peptides from transmembrane regions. *Nat. Methods* **2011**, *8*, 785–786.
- (16) Altschul, S. F.; Madden, T. L.; Schäffer, A. A.; Zhang, J.; Zhang, Z.; Miller, W.; Lipman, D. J. Gapped BLAST and PSI-BLAST: a new generation of protein database search programs. *Nucleic Acids Res.* **1997**, *25*, 3389–3402.

- (17) Nie, Z. J.; Hang, B. J.; Cai, S.; Xie, X. T.; He, J.; Li, S. P. Degradation of cyhalofop-butyl (CyB) by *Pseudomonas azotoformans* strain QDZ-1, and cloning of a novel gene encoding CyB-hydrolyzing esterase. *J. Agric. Food Chem.* **2011**, *59*, 6040–6046.
- (18) Zheng, X.; Chu, X.; Zhang, W.; Wu, N.; Fan, Y. A novel cold-adapted lipase from *Acinetobacter* sp. XMZ-26: gene cloning and characterisation. *Appl. Microbiol. Biot.* **2011**, *90*, 971–980.
- (19) Shabtai, Y.; Gutnick, D. L. Exocellular esterase and emulsan release from the cell surface of *Acinetobacter calcoaceticus*. *J. Bacteriol.* **1985**, *161*, 1176–1181.
- (20) Jansson, A.; Niemi, J.; Mäntsälä, P.; Schneider, G. Crystal structure of aclacinomycin methyltransferase with bound product analogues: implications for anthracycline recognition and mechanism. *J. Biol. Chem.* **2003**, *278*, 39006–39013.
- (21) Johnston, J. M.; Jiang, M.; Guo, Z.; Baker, E. N. Structural and functional analysis of Rv0554 from *Mycobacterium tuberculosis*: testing a putative role in menaquinone biosynthesis. *Acta Crystallogr., Sect. D: Biol. Crystallogr.* **2010**, *66*, 909–917.
- (22) Takeuchi, M.; Hamana, K.; Hiraishi, A. Proposal of the genus *Sphingomonas sensu stricto* and three new genera, *Sphingobium*, *Novosphingobium* and *Sphingopyxis*, on the basis of phylogenetic and chemotaxonomic analyses. *Int. J. Syst. Evol. Microbiol.* **2001**, *51*, 1405–1417.
- (23) Godoy, F.; Zenteno, P.; Cerda, F.; González, B.; Martínez, M. Tolerance to trichlorophenols in microorganism from pristine and polluted zone of the Biobío river (central Chile). *Chemosphere* **1999**, *38*, 655–662.
- (24) Arai, H.; Akahira, S.; Ohishi, T.; Kudo, T. Adaptation of *Comamonas testosteroni* TA441 to utilization of phenol by spontaneous mutation of the gene for a trans-acting factor. *Mol. Microbiol.* **1999**, *33*, 1132–1140.
- (25) Boon, N.; Goris, J.; De Vos, P.; Verstraete, W.; Top, E. M. Bioaugmentation of activated sludge by an indigenous 3-chloroaniline-degrading *Comamonas testosteroni* strain, I2gfp. *Appl. Environ. Microbiol.* **2000**, *66*, 2906–2913.
- (26) Boon, N.; Goris, J.; De Vos, P.; Verstraete, W.; Top, E. M. Genetic diversity among 3-chloroaniline- and aniline-degrading strains of the *Comamonadaceae*. *Appl. Environ. Microbiol.* **2001**, *67*, 1107–1115.
- (27) Hein, P.; Powlowski, J.; Barriault, D.; Hurtubise, Y.; Ahmad, D.; Sylvestre, M. Biphenyl-associated meta-cleavage dioxygenases from *Comamonas testosteroni* B-356. *Can. J. Microbiol.* **1998**, *44*, 42–49.
- (28) Dejonghe, W.; Berteloot, E.; Goris, J.; Boon, N.; Crul, K.; Maertens, S.; Hofte, M.; De Vos, P.; Verstraete, W.; Top, E. M. Synergistic degradation of linuron by a bacterial consortium and isolation of a single linuron-degrading *Variovorax* strain. *Appl. Environ. Microbiol.* **2003**, *69*, 1532–1541.
- (29) Radianingtyas, H.; Robinson, G. K.; Bull, A. T. Characterization of a soil-derived bacterial consortium degrading 4-chloroaniline. *Microbiology* **2003**, *149*, 3279–3287.
- (30) Yang, C. Y.; Li, Y.; Zhang, K.; Wang, X.; Ma, C. Q.; Tang, H. Z.; Xu, P. Atrazine degradation by a simple consortium of *Klebsiella* sp. A1 and *Comamonas* sp. A2 in nitrogen enriched medium. *Biodegradation* **2010**, *21*, 97–105.
- (31) Slater, J. H.; Lovatt, D. Biodegradation and the significance of microbial communities. In *Microbial degradation of organic compounds*; Gibson, D. T., Ed.; Marcel Dekker: New York, 1984; pp 439–485.
- (32) Taraban, R. H.; Berry, D. F.; Berry, D. A.; Walker, H. L. Degradation of dicamba by an anaerobic consortium enriched from wetland soil. *Appl. Environ. Microbiol.* **1993**, *59*, 2332–2334.
- (33) Gil, M.; Haïdour, A.; Ramos, J. L. Degradation of o-methoxybenzoate by a two-member consortium made up of a gram-positive *Arthrobacter* strain and a gram-negative *Pantotea* strain. *Biodegradation* **2000**, *11*, 49–53.
- (34) Manonmani, H. K.; Chandrashekaraiyah, D. H.; Sreedhar Reddy, N.; Elcey, C. D.; Kunhi, A. A. Isolation and acclimation of a microbial consortium for improved aerobic degradation of alpha-hexachlorocyclohexane. *J. Agric. Food Chem.* **2000**, *48*, 4341–4351.
- (35) Carvalho, M. F.; Alves, C. C. T.; Ferreira, M. I. M.; De Marco, P.; Castro, P. M. L. Isolation and initial characterization of a bacterial consortium able to mineralize fluorobenzene. *Appl. Environ. Microbiol.* **2002**, *68*, 102–105.
- (36) Sorensen, S. R.; Ronen, Z.; Aamand, J. Growth in coculture stimulates metabolism of the phenylurea herbicide isoproturon by *Sphingomonas* sp. strain SRS2. *Appl. Environ. Microbiol.* **2002**, *68*, 3478–3485.
- (37) De Souza, M. L.; Newcombe, D.; Alvey, S.; Crowley, D. E.; Hay, A.; Sadowsky, M. J.; Wackett, L. P. Molecular basis of a bacterial consortium: interspecies catabolism of atrazine. *Appl. Environ. Microbiol.* **1998**, *64*, 178–184.
- (38) Jaeger, K.; Dijkstra, B.; Reetz, M. Bacterial biocatalysts: molecular biology, three-dimensional structures, and biotechnological applications of lipases. *Annu. Rev. Microbiol.* **1999**, *53*, 315–351.